Molecular Modeling of Crystalline Oligothiophenes: Testing and Development of Improved Force Fields

Valentina Marcon and Guido Raos*

Dipartimento di Chimica, Materiali e Ingegneria Chimica "Giulio Natta", Politecnico di Milano, Via L. Mancinelli 7, 20131 Milano, Italy

Received: June 30, 2004; In Final Form: September 3, 2004

We present the results of an extensive test of different force field models for crystalline oligothiophenes. The models are mostly based on MM3 for intramolecular degrees of freedom, but they rely on ab initio calculations for the inter-ring torsion potential and the molecular charge distribution. The latter is represented using either point charges from a fit of the molecular electrostatic potential or atomic charges, dipoles, and quadrupoles from a distributed multipole analysis. The force fields are tested by comparing the experimental structures with static energy minimizations and, in a few cases, room-temperature molecular dynamics simulations, also. We find that the point-charge model yields satisfactory results for most systems, including α-tetrathiophene, α-sexithiophene, tetrahexylsexithiophene, and bis(dithienothiophene). However, α-perfluorosexithiophene represents one difficult case where the distributed multipole model turns out to be clearly superior. Finally, we find that it is necessary to rescale the MM3 van der Waals parameters when these are employed in molecular dynamics simulations to reproduce the correct crystal densities.

Introduction

The development of organic electronic and optoelectronic devices (field-effect transistors or FETs, light-emitting diodes or LEDs, large area displays, photovoltaic cells, organic lasers, etc.) is in many ways a mature research field.[1−5] A number of promising materials, including, in particular, oligo- and polythiophenes, have been identified[6−8]. Some devices have already reached the market as commercial products, and many more are expected in the near future. On the other hand, a considerable amount of research is still addressing very fundamental questions, such as the mechanisms of charge or excitation transport or the structure and properties of organic/metal interfaces. Understanding and being able to harness these phenomena should be very rewarding by allowing a more rational design and optimization of both materials and devices.

It is now recognized that many crucial properties, such as the mobilities and lifetimes of charge carriers and excitons, are very sensitive to intermolecular interactions and to the degree of structural order in the material and in the actual device.[1−5] It is fair to say that there is a sound qualitative understanding of the factors affecting them, such as the amount π-stacking and orbital overlap in the solid state or the orientation of these π-stacks with respect to the substrate in thin-film FETs. Tight molecular packing in the crystal is also expected to be associated with small reorganization energies upon electron or hole transfer, hence to greater charge mobilities.[10] However, there is still a lot of uncertainty and a lack of general principles on the best way to achieve these goals. Our control over supramolecular self-assembly or the formation of a particular crystal polymorph is still limited and rather primitive,[11,12] compared to our ability to design and synthesize conjugated molecules with a prescribed backbone structure, substitution pattern, chain length, and so forth. Some guiding principles are expected to come from comparative analyses of the crystal structures of π-conjugated systems, as in, for example, ref 13. Molecular modeling approaches may supply additional quantitative information and qualitative insights, much as electronic structure calculations have contributed to shaping our ideas about the factors affecting the conformation or the excitation spectrum of individual molecules, substituent effects, and so forth.[14−16]

This paper discusses the development and testing of an effective force field for crystalline oligothiophenes. Other authors have recently undertaken a similar program for condensed aromatics such as pentacene, which represent another important class of organic semiconductors.[17] Another recent example is the construction of very detailed and accurate models for chlorobenzenes, incoporating anisotropic atom−atom interactions derived from ab initio calculations.[18] Oligothiophenes are somewhat more complicated because of their backbone and (when present) side-chain flexibility, lower symmetry, and larger number of parameters. Our aim was to develop a model which is sufficiently accurate to describe the variety of structural features observed in oligothiophenes,[13] yet simple enough to be applied in large-scale molecular dynamics simulations of these materials. The inter-ring torsion potential, the representation of the molecular charge distribution, and the nonbonded van der Waals parameters were varied in a systematic way, using information from gas-phase ab initio calculations and comparing the results with crystallographic and (where available) thermochemical data. We validated our force fields using both energy minimizations and molecular dynamics simulations of the crystals.

In the following sections, we discuss our force field models and computational methods. Afterward, we apply them to the crystal forms of a few representative oligothiophenes (see Figure 1). These were selected to span the range from the classic herringbone arrangement of aromatic crystals (α-tetra- and α-sexithiophene,[19−21] T4 and T6), to π-stacked structures (α,α′-bis(dithieno[3,2-*b*:2′,3′-*d*]thiophene),[22] or BDT for short), to

* Corresponding author. E-mail: guido.raos@polimi.it. Phone: +39-02-2399-3051. Fax: +39-02-2399-3080.

10.1021/jp047128d CCC: $27.50
Published on Web 10/22/2004

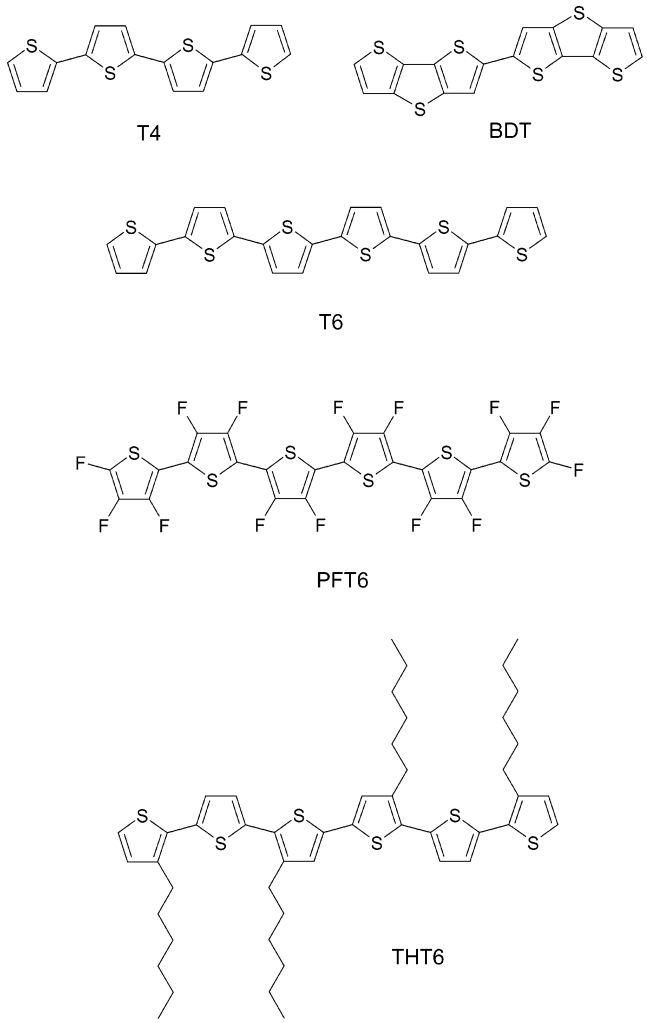

Figure 1. Structures of molecules considered in this study.

even more exotic packing modes (perfluorinated sexithiophene,[23] PFT6). We also consider the two polymorphs of 3,3″,4‴,3⁗-tetrahexyl-2,2′:5′,2″:5″,2‴:5‴,2⁗:5⁗,2⁗′:2⁗′-sexithiophene (THT6).[24,25] This compound is related to the important class of alkyl-substituted polythiophenes. These polymers display interesting polymorphism, but detailed structural models of their crystalline phases are still lacking (see ref 26 and references therein). Molecular modeling with a properly parametrized force field may represent a valuable addition to the experimental data, to gain a satisfactory understanding of these materials. The results for the unsubstituted T4 and T6 will be discussed in somewhat greater detail, because these results shaped our approach to the treatment of the other systems. The article ends with a summary of the main results and a discussion of more general issues and open problems.

Force Fields

Most of our simulations are based on the MM3 force field by Allinger and co-workers[27] and were carried out with the *TINKER 4.1* molecular modeling package.[28,29] The thiophene monomer had already been explicitly parametrized within MM3.[30] This particular study concerned gas-phase geometries and vibrational modes but, unlike the original papers on hydrocarbons,[27] did not address solid-state properties. The original parameters for the hard intramolecular degrees of freedom, namely bond stretching, bending, and most torsions, were thus adopted without modifications. The parameters for Buckingham's exp-6 nonbonded potential, representing repulsion−dispersion interactions between nonbonded atom pairs, were initially taken from the MM3 force field, but some modifications were included at a later stage (see text to follow). The models investigated and discussed here differ mostly by the representation of the soft inter-ring torsion potential and the molecular charge distributions. These are described in the following paragraphs.

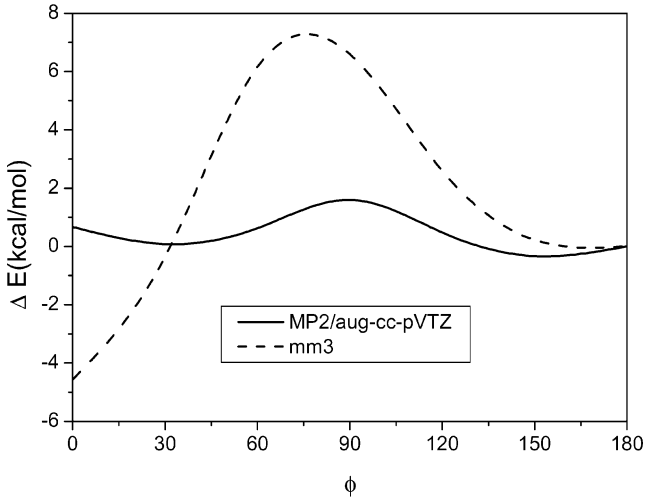

Figure 2. Comparison of the MM3 (- - -) and MP2/aug-cc-pVTZ (—) torsion potentials for 2,2′-bithiophene. Here, ϕ is the S−C_2−C_2′−S′ torsion angle. The trans planar state corresponds to $\phi = 180°$, the cis planar to $\phi = 0°$.

MM3. This is the standard MM3 parametrization with a torsion potential based on a semiempirical Pariser−Parr−Pople calculation of the inter-ring π-bond order and a description of molecular electrostatics based on bond dipoles.

MM3-T. This is the MM3 force field with the standard bond dipoles and a torsion potential based on high-level ab initio calculations (MP2/aug-cc-pVTZ) on 2,2′-bithiophene (T2).[31] The MM3 and ab initio torsion potentials of T2 are significantly different, as can be seen in the plots of Figure 2. MM3 predicts a torsional barrier that is too high at 90° and an energy that is too low for the cis planar state, compared to the reference trans planar state. However, these differences are not expected to have a major effect in the present case, because packing forces are sufficiently strong to keep most oligothiophenes close to a planar all-trans conformation in the crystals.

MM3-T-NoES. This is the MM3-T force field, with no electrostatic terms. Note that the importance of electrostatic interactions for aromatic crystal structures is widely recognized, and our calculations confirm this. Nonetheless, this model was investigated for comparison with a previous study using an MM2-based force field,[32] where the authors had noted that a model of T4 without electrostatic terms was actually performing better that a model including a crude description of electrostatics.

MM3-T-PDC. This is the MM3-T force field with potential-derived charges (PDC) on all atoms,[33] obtained from gas-phase B3LYP/6-31G** calculations on T4, BDT, and PFT4 in the trans planar conformations (C_{2h} symmetry), using the *GAMESS-USA* code.[34]

MM3-T-DM. This is the MM3-T force field with atom-centered charges, dipoles, and quadrupoles, obtained by a distributed multipole analysis[35−37] (DMA) of the B3LYP/6-31G** electron densities. By following the convention of *TINKER*', each set of Cartesian multipoles was transformed from the global to a local reference frame, defined by the atom on which they are centered and a suitable pair of atoms adjacent to it.

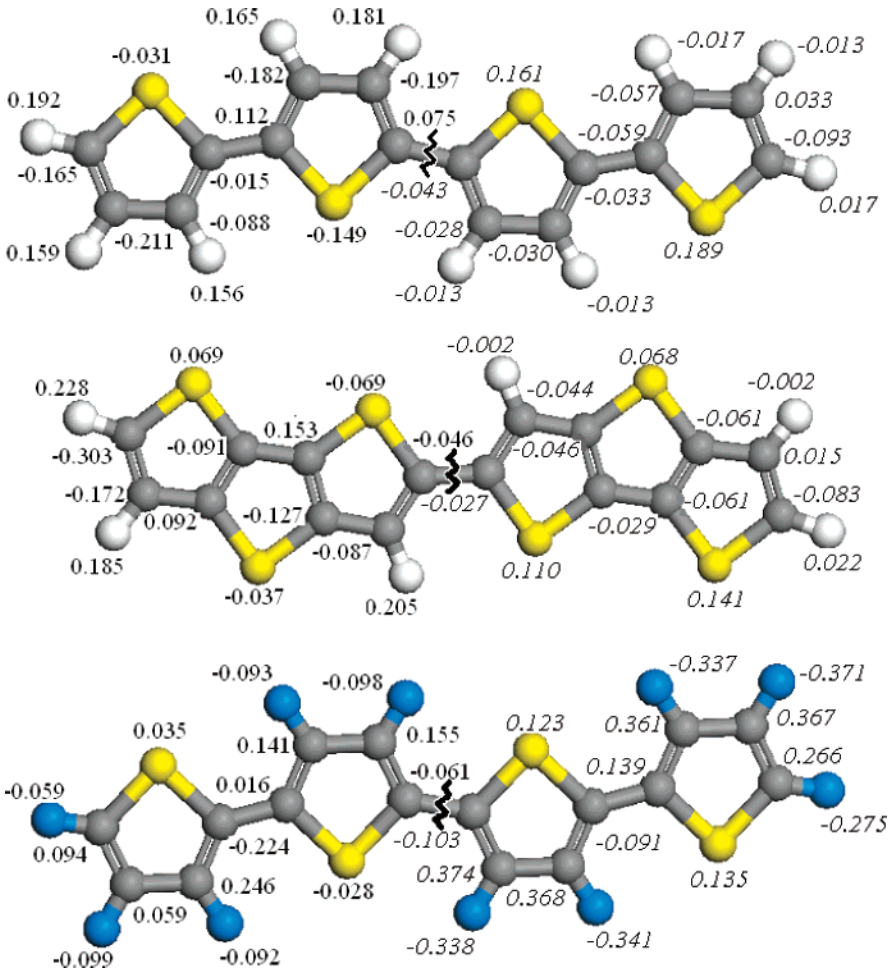

Figure 3. Graphical comparison of the charges of T4, BDT, and PFT4, obtained by the PDC (left-hand side, roman characters) and DMA (right-hand side, italics) analysis of the B3LYP/6-31G** electron densities.

MM3-T-PDC-C6. This is the MM3-T-PDC force field with an additional rescaling of all coefficients of the R^{-6} dispersion terms. The details and motivations for this rescaling will be given later in the text, in the discussion of the MD simulations.

For completeness, we shall also include in the discussion a rather different force field, which has been employed by us in a recent molecular dynamics study of T4 on a graphite surface:[38]

CFF91-T. This last case is the CFF91 force field of the *Materials Studio/Discover* package,[39] with the intrinsic torsion potential adjusted to reproduce the ab initio potential energy curve.[31] We point out that the atomic charges assigned by CFF91 on the basis of a simple bond incremental scheme are rather similar to the PDC charges from the B3LYP/6-31G** calculations.[38]

It is worth stressing that the intrinsic torsion potential entering a given force field is conceptually different from the ab initio one, because the latter represents a total energy difference which implicitly includes inter-ring nonbonded interactions and, to a lesser degree, the stretching and bending terms also. Therefore, the intrinsic potential was not simply exported from MM3-T to MM3-T-PDC or the other force fields without modifications. Rather, it was readjusted for each different nonbonded interaction model, with the aim of reproducing the same ab initio potential energy curve after inclusion of all the other force field terms.

Comparison of the ab initio charges and multipoles reveals a good degree of transferability over chemically similar sites. This is illustrated in Figure 3, for the PDC and DMA charges (monopoles) of T4, BDT, and PFT4 (perfluorinated tetrathiophene). Preliminary checks even demonstrated that averaging over chemically similar sites did not produce major differences in the optimized crystal structures. Eventually, we retained the original charges or multipoles for the sake of accuracy. However, we exploited this transferability by using the charges or multipoles of T4 and PFT4 for the higher oligomers also. More precisely, the four inner rings of the T6 and PFT6 were parametrized on the basis of the two inner rings of the tetramers. Also, for consistency with the philosophy of MM3 of not having any bond dipoles on $C(sp^3)-C(sp^3)$ and $C(sp^3)-H$ bonds, our modified electrostatic models for alkylthiophenes did not include any charges or higher multipoles on the side chains. The only exception was represented by the C atoms directly bonded to the thiophene rings, where these parameters were directly taken from those of the corresponding H atoms in the unsubstituted compound, so as to retain strict electroneutrality.

It is interesting to compare the electrostatic potential (ESP) charges and the first-order terms (monopoles) from the DMA. Looking again at Figure 3, we see that the sulfurs of T4 and BDT are positive according to DMA, negative according to ESP. Also, the DMA charges on the carbons and hydrogens are nearly zero (typically ± 0.05 e), whereas ESP charges are larger (typically ± 0.2 e), with positive values on H and negative values on C. These differences can be understood by recognizing that the ESP charges try to mimic the characteristic sandwich-like electrostatic field of aromatic systems, which is positive in the plane of the ring but negative above and below it. In a distributed multipole picture, this effect is modeled mainly by the Θ_{zz}

component of the atomic quadrupoles (assuming that the rings lie in the *xy* plane), and the atomic charges can take smaller values in this case. In PFT4, the carbons are positive and the fluorines negative, as expected. However, now the DMA charges are larger (in absolute values) than the ESP values.

The quality of the point-charge approximation can be judged by looking at the root mean square (rms) deviation between the reference and the fitted electrostatic energies

$$\Delta = e \times \sqrt{\frac{1}{N}\sum_{i=1}^{N}[\phi_{\mathrm{fit}}(i) - \phi_{\mathrm{ref}}(i)]^2} \qquad (1)$$

The absolute errors for T4, BDT, and PFT4 are comparable (0.90, 1.34, and 1.04 kcal/mol, respectively; the number of points is always $N \approx 2000$). However, the relative deviations

$$\delta\% = 100 \times \sqrt{\sum_{i=1}^{N}[\phi_{\mathrm{fit}}(i) - \phi_{\mathrm{ref}}(i)]^2 \Big/ \sum_{i=1}^{N}[\phi_{\mathrm{ref}}(i)]^2} \qquad (2)$$

are significantly different, being respectively equal to 14.8%, 21.8%, and 33.5%. Hence, the point-charge approximation is expected to be more satisfactory for T4 than for PFT4. This is borne out by the simulations, as we shall see.

Simulation Details

We performed both static energy minimizations and room-temperature molecular dynamics (MD) simulations of the crystals.[40,41] In the energy minimizations, van der Waals interactions were smoothly reduced to zero beyond the default cutoff of 9.0 Å, while the electrostatic interactions were calculated exactly by Ewald summation. Two kinds of energy minimizations were performed. In the first, cell parameters were fixed at the experimental values, and only the atomic coordinates were allowed to change (these will be referred to as atoms-only minimizations). To this purpose, we employed the *NEWTON* program of *TINKER* with the default options, which implements a truncated Newton optimization algorithm. A second set of minimizations (hencefort called full-cell) was carried out with the *XTALMIN* program, which performs a full-crystal energy minimization by alternating cycles of truncated Newton optimization over atomic coordinates with variable metric optimization over the lattice dimensions and angles. In both cases, the rms gradient at convergence was set to 0.0001 kcal mol^{-1} Å^{-1}. The heats of sublimation were simply calculated from the difference in potential energy per mole of molecules in the crystal and gas phases (the latter from single-molecole optimizations)

$$\Delta H^{\circ}_{\mathrm{subl}} \approx U_{\mathrm{gas}} - U_{\mathrm{cryst}}$$

The *RT* term ($=p\Delta V$), which is sometimes included in the right-hand side, is only 0.6 kcal/mol at 300 K. This is smaller than the experimental uncertainties for T4 and T6 and accounts for a modest 2−3% of their heats of sublimation.

Three different figures of merit were used judge the quality of the optimized structures. The first one is the dimensionless structural drift factor *F*, which quantifies the overall translation-rotation of the molecules and changes in the unit cell[42−44]

$$F = (\Delta x/0.1\ \text{Å})^2 + (\Delta\phi/2)^2 + (100\Delta a/a)^2 + (100\Delta b/b)^2 + (100\Delta c/c)^2 + \Delta\alpha^2 + \Delta\beta^2 + \Delta\gamma^2 \qquad (3)$$

Here, Δx and $\Delta\phi$ represent the translation of the center of mass of the molecules and the rotation of the principal axes of inertia with respect to the experimental positions, while $\Delta a,\ldots,\Delta\gamma$ are the differences between the calculated and experimental lattice constants. The figures of merit Δ_{cell} and Δ_{mol} measure the mean-square displacements of the heavy atoms (i.e., neglecting hydrogens). Δ_{cell} is simply the difference between the starting (i.e., experimental) and optimized atomic coordinates, within a rigid crystal lattice (i.e., for the atoms-only minimizations). This quantity includes contributions from translation-rotation of the molecules (like *F*), but also from changes in molecular geometry. Δ_{mol} attempts to quantify only the latter (intramolecular distortion), by measuring the mean-square displacements after translating and rotating the symmetrical unit of the cell (typically one or one-half of a molecule) to bring its center of mass and principal axes of inertia to coincide with those in the experimental structures.

Molecular dynamic simulations of the crystals were carried out in the *NPT* ensemble. A 12.0 Å cutoff was adopted for the evaluation of both van der Waals and electrostatic interactions. All of the simulated systems were built from the unit cell, which was replicated in the three directions of space in order to obtain a supercell with all axes at least double the cutoff distance. The "loose-coupling" method by Berendsen et al.[45] was used to control both temperature and pressure, which were set to 300 K and 0.0 atm, respectively. The *DYNAMIC* program of *TINKER* was modified in order to allow independent (i.e., nonisotropic) fluctuations of all cell parameters, following the original treatment.[45] The default relaxation times $\tau_T = 0.2$ ps and $\tau_P = 2$ ps were used for the thermostat and barostat. The equations of motion were integrated by the Velocity Verlet algorithm with a 1 fs time step. The simulations lasted 500 ps, of which the first 100 ps were discarded from the analysis in order to allow proper equilibration. Atomic coordinates were saved to disk every 10 ps for later analysis.

Results and Discussion

Tetrathiophene (T4): Energy Minimizations. Two distinct polymorphs of T4 have been produced and characterized experimentally, first by powder[19] and afterward by single-crystal[20] X-ray diffraction. They are often identified as low temperature (LT) or high temperature (HT), depending on the temperature range of the source in crystal growth by vapor deposition. In both structures, the molecules are exactly or nearly planar and adopt a typical herringbone packing (see Figures 4 and 5). The two forms belong to different variants of the same space group ($P2_1/c$ and $P2_1/a$, respectively), but the former has a lower symmetry, because it contains one independent molecule per unit cell, while the second has only one-half of a molecule as the independent unit (the crystallographic inversion center coincides with the molecular center of symmetry). Therefore, the volume of the LT unit cell is double that of the HT cell, their experimental densities being nearly identical.

Ferro et al.[32] used a modified MM2 force field to model the unit cell of the LT crystals. These calculations produced interesting qualitative insights, for example, into the reasons for the lack of intramolecular symmetry in this polymorph. However, they were unable to describe the crystal structure in quantitative detail, so that full simultaneous optimization of the atomic coordinates and of the unit cell parameters led to unacceptably large deviations from the experimental structure. This was ascribed to the crude representation of the molecular charge distribution (dipoles only on the C−S bonds), and indeed, agreement with experiment improved by switching off all electrostatic interactions.

TABLE 1: Minimization Results for the LT Form of T4[a]

	experiment	MM3	MM3-T	MM3-T-NoES	MM3-T-PDC	MM3-T-PDC-C6	MM3-T-DM	CFF91-T
				Atoms Only				
Δ_{mol} (Å)		0.145	0.112	0.097	0.103	0.106	0.113	0.234
Δ_{cell} (Å)		0.288	0.494	0.260	0.269	0.284	0.269	0.432
F		2.824	6.761	2.304	2.184	2.224	2.485	4.351
ϕ_1, ϕ_3 (°)	178.4, 179.6	172.1, 173.6	177.0, 179.2	176.9, 177.5	176.1, 179.3	173.8, 179.5	176.4, 177.4	167.8, 168.3
ϕ_2 (°)	179.8	170.7	178.8	178.4	178.3	177.6	178.2	179.8
				Full Cell				
a (Å)	6.085	6.536	6.218	6.511	5.977	5.929	6.417	5.695
b (Å)	7.858	7.474	7.638	7.358	7.974	7.612	7.396	7.525
c (Å)	30.483	30.933	31.372	31.372	31.118	30.851	31.641	34.024
β (°)	91.810	91.621	90.954	92.810	89.178	89.059	93.417	105.476
ρ (g/cm^3)	1.504	1.451	1.471	1.473	1.478	1.574	1.462	1.559
Δ_{mol} (Å)		0.211	0.120	0.121	0.109	0.104	0.121	0.215
F		96.94	29.08	117.94	17.85	32.29	98.12	4248.0
ϕ_1, ϕ_3 (°)	178.4, 179.6	165.1, 168.9	176.5, 179.6	175.6, 176.7	177.9, 178.2	177.5, 178.4	175.7, 177.8	171.5, 174.0
ϕ_2 (°)	179.8	163.7	179.8	180.0	179.6	179.5	179.7	179.1
$\Delta H°_{subl}$ (kcal/mol)	33.4 ± 1.6	29.580	30.247	27.840	29.857	40.171	28.234	27.633

[a] Δ_{mol}, Δ_{cell}, and F have been described in the main text. a, b, c, and β are the lattice parameters for a monoclinic unit cell. ϕ_1, ϕ_2, and ϕ_3 are the S−C−C−S torsion angles along the molecular backbone. Space group is $P2_1/c$ ($Z = 4$).

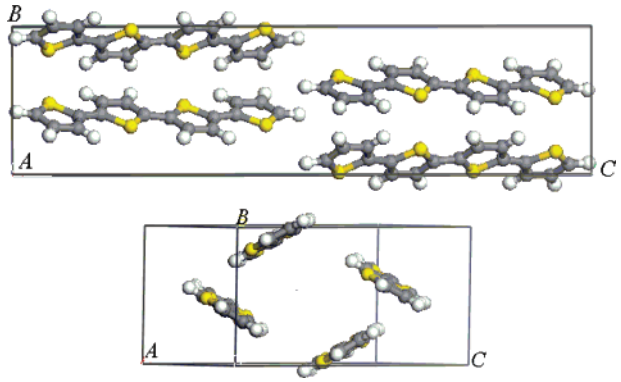

Figure 4. Two views of the unit cell of the LT form of T4 (from MM3-T-PDC full-cell minimization).

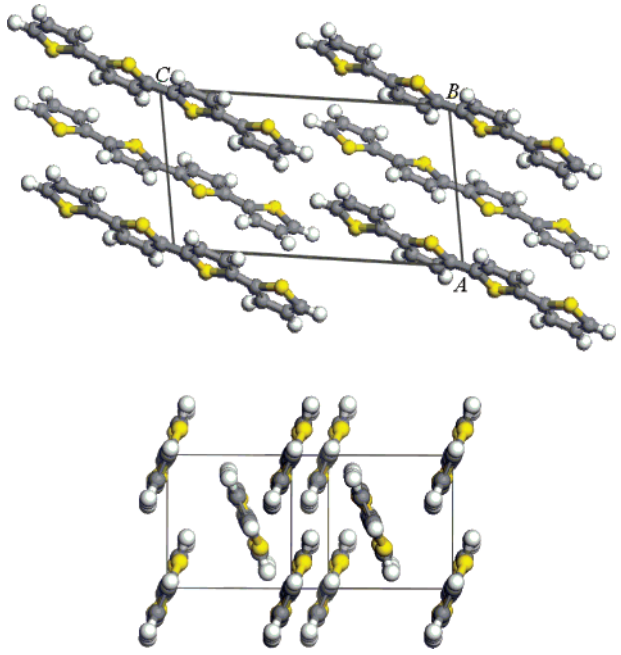

Figure 5. Two views of the unit cell of the HT form of T4 (from MM3-T-PDC full-cell minimization).

Table 1 summarizes our energy minimization results on the LT polymorph. The atoms-only optimizations do not discriminate clearly between the different force fields, because F, Δ_{cell}, and Δ_{mol} take rather similar values in all cases (the F value for MM3-T appears to be the only exception). The only difference that is worthwhile noting is that MM3 and CFF91-T lead to slightly more conformationally distorted molecules (average S−C−C′−S′ ϕ torsion angles around 170°), while the other force fields lead to almost planar molecules, with all angles $\phi \geq 176°$. Instead, major differences among the force fields are highlighted by the full-cell minimizations. The F values for the MM3-based force fields are in the range between 18 (MM3-T-PDC) and 119 (MM3-T-NoES). The densities are slightly lower than experimental values, except (somewhat unsurprisingly) for MM3-T-PDC-C6, which includes larger dispersion interactions. The results are far worse for CFF91-T ($F = 4248$) because of very large changes (>10%) of the c axis and the β angle. Visual inspection on the minimized unit cell also reveals that in this case the molecules almost lose the herringbone packing to adopt a more π-stacked arrangement.

The corresponding results for the HT polymorph are given in Table 2. Again, the atoms-only minimizations yield relatively small differences in Δ and F, with MM3-T-PDC performing best and CFF91-T worst. Note that the central torsion is exactly 180° because of the intramolecular symmetry element, and also, the two outer ones are always nearly trans planar. Surprisingly, CFF91-T turns out to be the best force field in the full-cell minimizations. We believe this result to be fortuitous, however, considering the poor performance of the force field in the other tests. On the other hand, MM3-T-PDC consistently remains the best among the MM3-based parametrizations.

It is interesting to note that the results of the atoms-only minimizations (Δ_{cell} or F values) cannot be used to predict the performance of a force field in the more demanding full-cell minimizations (F value). Thus, MM3-T-NoES is among the best in the atoms-only minimization of the LT form, but it is actually the worst (with the exception of CFF91-T) in the full-cell minimization. Conversely, CFF91-T is the worst in the atoms-only minimization of the HT form, but turns out to be the best performer in the full-cell minimization.

With the sole exception of MM3-T-PDC-C6, the different force fields lead to rather similar estimates of the packing energies of the LT and HT crystals (see the heats of sublimation in Tables 1 and 2). The similarity among the force fields in predicting the energies of a given polymorph depends mainly on the smallness of the electrostatic contribution to the lattice energy. In turn, this is proven by the fact that the MM3-T-

TABLE 2: Minimization Results for the HT Form of T4[a]

	experiment	MM3	MM3-T	MM3-T-NoES	MM3-T-PDC	MM3-T-PDC-C6	MM3-T-DM	CFF91-T
				Atoms Only				
Δ_{mol} (Å)		0.100	0.105	0.110	0.103	0.106	0.104	0.101
Δ_{cell} (Å)		0.179	0.177	0.194	0.161	0.161	0.190	0.223
F		3.883	3.935	4.320	1.936	1.703	4.261	9.853
ϕ_1, ϕ_3 (°)	179.1	178.0	177.9	177.6	178.4	178.4	178.0	179.8
				Full Cell				
a (Å)	8.935	8.367	8.394	8.005	8.348	7.992	8.312	8.951
b (Å)	5.751	5.974	5.960	6.165	5.942	5.843	6.079	5.563
c (Å)	14.340	14.968	14.973	15.243	15.049	15.015	14.958	14.113
β (°)	97.22	98.95	98.76	98.63	98.43	98.48	99.14	94.279
ρ (g/cm^3)	1.499	1.484	1.482	1.475	1.486	1.582	1.471	1.566
Δ_{mol} (Å)		0.112	0.117	0.115	0.121	0.120	0.121	0.102
F		92.265	85.642	201.800	89.361	151.043	125.691	28.568
ϕ_1, ϕ_3 (°)	179.1	177.6	177.7	175.5	177.9	176.9	175.7	179.9
$\Delta H°_{subl}$ (kJ/mol)	33.4 ± 1.6	30.493	31.308	28.262	29.542	39.866	28.364	27.765

[a] Space group is $P2_1/a$ ($Z = 2$). Central torsion angle is $\phi_2 = 180°$ exactly, for symmetry reasons. See also the caption to Table 1.

TABLE 3: Average Lattice Parameters from Molecular Dynamics Simulations with the MM3-T-PDC−C6 Force Field[a]

	4TLT (*)	4TLT	4THT (*)	4THT	6TLT	6THT	THT6-Y	THT6-R
a (Å)	6.020 (−1.1%)	5.880 (−3.4%)	8.743 (−2.1%)	8.207 (−8.1%)	45.181 (+1.1%)	8.109 (−11%)	5.833 (+6.2%)	25.412 (+1.8%)
b (Å)	8.528 (+8.5%)	8.100 (+3.1%)	5.995 (+4.2%)	5.936 (+3.2%)	8.060 (+2.7%)	5.977 (+5.1%)	13.274 (−2.2%)	7.844 (+4.4%)
c (Å)	31.152 (+2.2%)	30.873 (+1.3%)	15.341 (+7.0%)	15.155 (+5.7%)	5.878 (−2.8%)	22.033 (+6.6%)	16.431 (−0.1%)	13.549 (−2.3%)
α (°)	90.00	90.00	90.00	90.00	90.00	90.00	99.61 (−2.8%)	90.00
β (°)	88.81 (−3.3%)	88.29 (−3.8%)	95.28 (−2.0%)	97.43 (+0.2%)	87.54 (−3.5%)	95.69 (−2.1%)	92.36 (−0.2%)	115.00 (−1.9%)
γ (°)	90.00	90.00	90.00	90.00	90.00	90.00	104.00 (+3.1%)	90.00
ρ (g/cm^3)	1.372 (−8.8%)	1.491 (−0.9%)	1.369 (−8.7%)	1.497 (−0.1%)	1.534 (+1.1%)	1.544 (+0.1%)	1.137 (−2.8%)	1.127 (−5.4%)

[a] Relative deviations from the experimental values are indicated in parentheses. Asterisk (*) refers to simulations with the MM3-T-PDC force field. All simulations conducted at 300 K and 0 atm. Actual lattice parameters of the MD supercell are multiples of the a, b, and c axes given in the table.

NoES heats of sublimation are only ∼2 kcal/mol smaller than the other models. Indeed, it is generally recognized that electrostatics imparts directional character to intermolecular interactions, but most of the net attraction energy comes from dispersion forces.[35] The substantial increase in going from MM3-T-PDC to MM3-T-PDC-C6 (∼33%) is comparable to the scaling factor for the individual van der Waals interaction energies (∼39%, see text to follow). Interestingly, the experimental heat of sublimation of T4[46] (presumably for the LT form, because the HT polymorph was only discovered shortly afterward) falls between these two values. Finally, all force fields yield very similar packing energies for the two polymorphs. Note that MM3-T-PDC and MM3-T-PDC-C6 predict the LT form to be more stable by ∼0.3 kcal/mol, whereas the other force fields predict the HT form to be slightly favored.

Molecular Dynamics of T4: Calibration of the Exp-6 Potentials. Because the experimental crystal structures were obtained at room temperature,[20] comparison with room-temperature MD simulations is more rigorously correct than comparison with static energy minimizations. It is worth reminding the reader that organic crystals have temperature expansion coefficients on the order of 2×10^{-4} K^{-1},[12] so that one typically expects a 6% increase in volume when going from 0 to 300 K. Conversely, a minimized crystal structure should be approximately 6% denser than experimental results, when the latter is obtained at room temperature.

In view of the good performance of the simple point-charge model in the static energy minimizations, this was adopted for all MD simulations. The results for the two forms of T4 with the MM3-T-PDC force field are given in Table 3. As can be seen, these tend to produce densities that are too low (approximately 9% below the experimental value). This, coupled with the fact that the same force field tends to underestimate the heats of sublimation (see Tables 1 and 2), suggested the need to increase the well depth and decrease the minimum energy distance for some or all nonbonded interactions. Modification of the exp-6 parameters for the dispersion−repulsion interactions was almost forced upon us by the fact that the densities and the heats of sublimations are almost unaffected by the choice of the electrostatic model. Comparison of the MM3 potentials (see plots in the Supporting Information) with other widely used exp-6 potentials (namely those of Mirsky[35] and of Gavezzotti and Filippini[44]) or with the Lennard-Jones potentials of the OPLS-AA force field[47] shows that the former are systematically lower than the latter, so that there is certainly room for a limited modification of the potentials in this direction. There are, of course, many ways to do this, because there are at least six parameters associated with the H, C(sp^2), and S atom types (see text to follow). A full re-parametrization goes beyond the purpose of our study and would, in any case, require a much larger number of compounds and experimental data. The brute force adoption of another set of exp-6 potentials on top of the MM3 force field was also considered unsatisfactory. Therefore, we undertook a limited re-parametrization of the MM3 exp-6 potentials, with the general strategy of (a) making the least possible changes to the

TABLE 4: Minimization Results for the LT Form of T6[a]

	experiment	MM3	MM3-T	MM3-T-NoES	MM3-T-PDC	MM3-T-PDC-C6	MM3-T-DM	CFF91-T
				Atoms Only				
Δ_{mol} (Å)		0.269	0.285	0.229	0.132	0.187	0.231	0.299
Δ_{cell} (Å)		0.944	0.941	0.744	0.256	0.312	0.758	0.693
F		18.526	27.773	15.480	1.483	1.702	16.256	12.891
ϕ_1, ϕ_5 (°)	179.2, 179.6	175.0, 177.4	179.0, 179.1	178.9, 179.4	178.1, 178.4	174.6, 178.4	178.9, 179.2	168.2, 169.2
ϕ_2, ϕ_4 (°)	179.5, 179.8	176.1, 177.6	178.3, 178.6	178.5, 178.8	177.2, 179.3	176.9, 177.7	178.3, 178.7	177.1, 177.3
ϕ_3 (°)	179.9	178.9	174.7	175.6	179.9	178.8	175.7	179.9
				Full Cell				
a (Å)	44.708	45.399	45.944	45.877	45.509	45.099	46.274	49.836
b (Å)	7.851	7.528	7.653	7.436	7.972	7.644	7.431	7.497
c (Å)	6.029	6.473	6.195	6.436	5.974	5.912	6.381	5.743
β (°)	90.76	90.58	90.53	91.66	88.43	87.89	92.52	106.28
ρ (g/cm^3)	1.551	1.483	1.506	1.495	1.515	1.611	1.497	1.593
Δ_{mol} (Å)		0.234	0.176	0.171	0.156	0.162	0.174	0.311
F		85.995	28.425	81.734	17.191	21.707	95.834	488.711
ϕ_1, ϕ_5 (°)	179.2, 179.6	167.5, 169.1	177.2, 179.2	176.1, 176.6	178.0, 179.1	178.2, 178.6	176.1, 177.5	169.0, 169.0
ϕ_2, ϕ_4 (°)	179.5, 179.8	164.6, 165.6	179.3, 179.9	178.5, 178.7	179.2, 179.7	179.3, 179.7	178.6, 179.2	177.4, 177.4
ϕ_3 (°)	179.9	164.6	178.2	178.9	179.1	179.1	178.8	180.0
ΔH°_{subl} (kcal/mol)	50.0 ± 0.5	42.867	44.572	41.057	44.494	59.568	41.701	42.179

[a] Space group is $P2_1/n$ ($Z = 4$). See also the caption to Table 1.

individual parameters and (b) keeping the size of parameter space to a minimum.

The repulsion−dispersion interactions between a pair of nonbonded atoms are represented within the MM3 force field by the standard functional form[27]

$$V(r) = \epsilon\left\{A\exp\left[-B\left(\frac{r}{r_0}\right)\right] - C\left(\frac{r}{r_0}\right)^6\right\} \qquad (4)$$

A, B, and C are adimensional constants, taking the values $A = 184\,000$, $B = 12.0$, and $C = 2.25$ for all possible interactions. They are such that r_0 represents the position of the potential energy minimum for a specific pair of atoms, and the well depth is $V_{min} = -1.120\epsilon$. The MM3 values are $r_0 = 3.24$ Å and $\epsilon = 0.0837$ kJ/mol for H, $r_0 = 3.92$ Å and $\epsilon = 0.2343$ kJ/mol for C(sp^2), and $r_0 = 4.3$ Å and $\epsilon = 0.8452$ kJ/mol for S. Cross-interactions are simply dealt with by taking the arithmetic average of the r_0's and the geometric average of the ϵ's.

We experimented with a number of options, including a modification of the r_0 and ϵ parameters for the interactions involving sulfur. The H···H, C···C, and C···H potentials were initially left unchanged, because they were considered to be more thoroughly tested and consolidated. Acceptable results for the room-temperature densities were obtained only by doubling the well depth of sulfur and, to a lesser extent, a concomitant shortening of its radius. These parameters are not altogether unrealistic, because this S···S interaction would be comparable to that embodied by the Gavezzotti−Filippini potentials (see again the plots in the Supporting Information). However, this strategy was eventually abandoned, because such a major modification for a single element would probably result in an unbalanced description or, in any case, limit its transferability to other molecular systems. A more even, less invasive rescaling of all the nonbonded parameters was considered preferable. Eventually, we decided to leave all of the ϵ's and r_0's unchanged and rescale all interactions (including those for C and H) by increasing the C coefficient in eq 1. In doing so, we reasoned that these conjugated systems should be more polarizable than their nonconjugated analogues, and hence, they would experience greater dispersion interactions. We experimented with a few values in the range 2.25−3.0 and finally chose $C = 2.65$. With this particular value, the potential minima fall at $r_{min} = 0.968r_0$ and have a value of $V_{min} = -1.561\epsilon$ (i.e., 39% deeper than the original MM3 values).

The room-temperature densities and lattice parameters with the resulting MM3-T-PDC-C6 force field are in good agreement with the experimental values for the LT crystals (see Table 3). The density of the HT crystals is also correct, but unfortunately, this is achieved at the price of larger individual distortions of the a and c axes. Also, the heats of sublimation are somewhat overestimated by the MM3-T-PDC-C6 force field (see again Tables 1 and 2). Nonetheless, we decided to emphasize the densities and crystallographic data over the thermal data in selecting the final form of the nonbonded parameters, also in view of the smaller margin of error for the former.

Sexithiophene (T6). Two distinct polymorphs, analogous by structure and symmetry to the LT and HT forms of T4, have been identified also in the case of T6.[19,21] Also, our minimization results, which are collected in Tables 4 and 5, closely parallel those of T4 and may be summarized by saying that MM3-T-PDC appears to provide the best overall representation of the two polymorphs. CFF91-T is even better for the HT form but fails badly for the LT form. The fact that MM3-T-NoES performs worst among all MM3-based force field confirms an established fact, namely, that electrostatic interactions are an important player in determining the crystal structures of seemingly nonpolar aromatic systems. On the other hand, the relatively poor performance of the more sophisticated MM3-T-DM model is somewhat unexpected, although it has been observed before in a number of (but by no means all) cases.[48]

Room-temperature MD simulations confirm the need to rescale the original van der Waals parameters in order to reproduce the experimental densities (Table 3). The individual lattice parameters of the LT form are well reproduced by the MM3-T-PDC-C6 force field, unlike those of the HT form, which are less satisfactory.

In the following sections, we shall examine in turn the remaining crystal structures (the two polymorphs of THT6, BDT, and PFT6). In view of the results for T4 and T6, we decided to concentrate on the MM3-T-PDC and MM3-T-DM force fields and, for the MD simulations, also MM3-T-PDC-C6.

Tetrahexylsexithiophene (THT6). The placement of appropriate substituents along the chain backbone represents a convenient and effective way to tune the properties (electronic,

TABLE 5: Minimization results for the HT Form of T6[a]

	experiment	MM3	MM3-T	MM3-T-NoES	MM3-T-PDC	MM3-T-PDC-C6	MM3-T-DM	CFF91-T
				Atoms Only				
Δ_{mol} (Å)		0.133	0.128	0.141	0.139	0.137	0.134	0.161
Δ_{cell} (Å)		0.172	0.171	0.189	0.165	0.166	0.187	0.299
F		2.761	2.757	2.729	1.177	0.976	2.714	6.747
ϕ_1, ϕ_5 (°)	178.9	177.8	177.7	177.3	177.8	177.6	177.5	179.7
ϕ_2, ϕ_4 (°)	179.9	179.2	179.3	179.2	179.1	179.0	179.2	179.7
				Full Cell				
a (Å)	9.140	8.481	8.484	8.279	8.783	8.159	8.712	9.081
b (Å)	5.684	6.006	6.008	6.169	5.840	5.851	6.012	5.565
c (Å)	20.672	21.260	21.242	21.343	21.238	21.263	20.937	20.659
β (°)	97.78	93.96	93.88	93.10	94.74	93.05	93.84	100.735
ρ (g/cm^3)	1.542	1.518	1.519	1.507	1.511	1.618	1.499	1.599
Δ_{mol} (Å)		0.156	0.154	0.153	0.158	0.151	0.159	0.158
F		127.509	127.795	193.924	44.502	154.315	91.034	19.928
ϕ_1, ϕ_5 (°)	178.9	176.9	177.2	174.8	176.8	175.8	175.0	179.7
ϕ_2, ϕ_4 (°)	179.9	179.1	179.7	179.2	178.6	178.6	178.7	179.8
$\Delta H°_{subl}$ (kcal/mol)	50.0 ± 0.5	44.402	46.337	41.641	43.847	59.067	41.667	42.798

[a] Space group is $P2_1/a$ ($Z = 2$). Central torsion angle is $\phi_3 = 180°$ exactly, for symmetry reasons. See also the caption to Table 1.

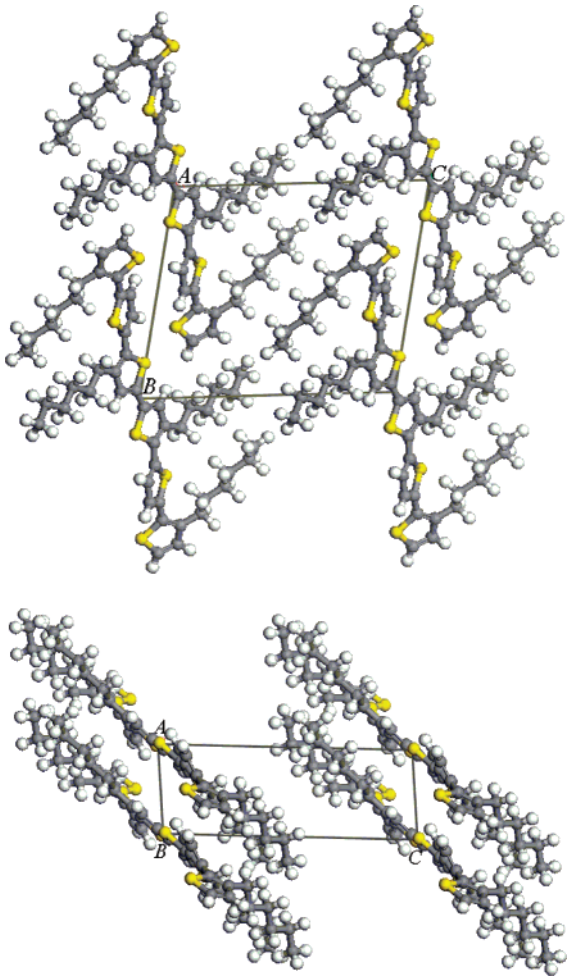

Figure 6. Two views of the unit cell of the yellow form of THT6 (from MM3-T-PDC full-cell minimization).

optical, self-assembly, interaction with substrates, processability, etc.) of organic semiconductors. Consequently, many substituted oligothiophenes have been synthesized and tested, and for a number of these, the crystal structures have been determined. Pendant alkyl chains are particularly important because of their ability to improve solubility and processability without degrading the electronic properties. Oligoalkylthiophenes are also important as model compounds for the structure of the alkyl-substituted polymers.

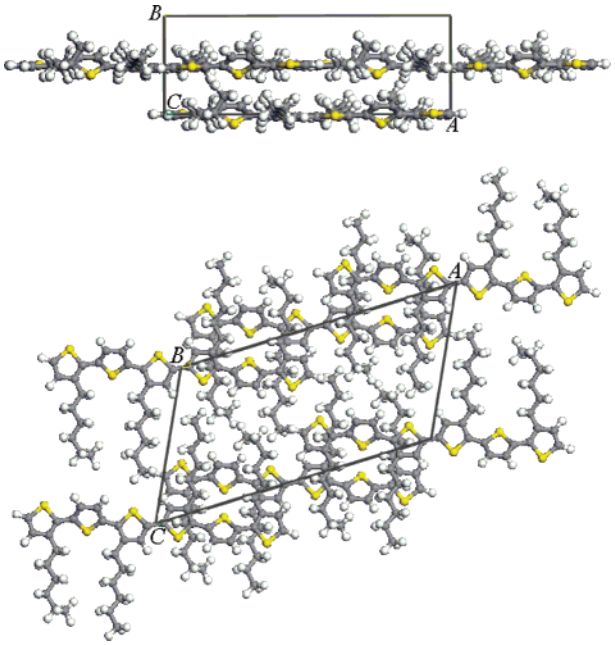

Figure 7. Two views of the unit cell of the red form of THT6 (from MM3-T-PDC full-cell minimization).

Two crystalline forms of THT6 have been produced and characterized by Porzio and co-workers, namely, the so-called yellow[24] and red[25] polymorphs (see Figures 6 and 7). The structure of the yellow form was obtained by single-crystal X-ray diffraction. Unlike the other oligothiophene structures, it has a triclinic unit cell ($P1$ group) and a non-coplanar arrangement of the thiophene backbone. The alkyl side chains are not interdigitated. They are mostly trans planar, except for the first bond of the two outer side chains (χ_{11} and χ_{61}, following the notation of ref 24) which are in a gauche conformation (Table 6). The Δ_{cell} values from atoms-only minimizations are all very similar and almost identical to those reported by Destri et al.[24] using their MM2-type force field.[32] Both the main-chain and the backbone torsion angles remain very close to the experimental values. The unit cell parameters from the full-cell minimizations remain very close to the experimental values. Now, the distributed multipole model is marginally better that the point-charge one. Perhaps surprisingly, its performance is actually better than for the two polymorphs of unsubstituted T6 (compare the F values).

TABLE 6: Minimization Results for the Yellow Form of THT6[a]

	experiment	MM3-T-PDC	MM3-T-PDC-C6	MM3-T-DM
		Atoms Only		
Δ_{mol} (Å)		0.186	0.158	0.179
Δ_{cell} (Å)		0.188	0.180	0.187
F		0.125	0.191	0.113
$\phi_1, -\phi_5$ (°)	137.3	134.5	133.9	135.8
$-\phi_2, \phi_4$ (°)	165.7	162.3	162.2	162.8
$\chi_{11}, -\chi_{61}$ (°)	77.5	76.6	76.8	77.6
$\chi_{31}, -\chi_{41}$ (°)	1.2	2.7	1.9	4.2
		Full Cell		
a (Å)	5.492	5.631	5.455	5.418
b (Å)	13.578	13.625	13.406	13.686
c (Å)	16.453	16.016	15.864	16.603
α (°)	102.460	100.13	99.80	100.28
β (°)	92.540	93.28	84.51	92.54
γ (°)	100.860	97.25	97.88	97.77
ρ (g/cm^3)	1.174	1.223	1.223	1.151
Δ_{mol} (Å)		0.411	0.188	0.476
F		30.665	37.673	20.394
$\phi_1, -\phi_5$ (°)	137.3	133.0	134.4	135.9
$-\phi_2, \phi_4$ (°)	165.7	161.1	162.6	162.7
$\chi_{11}, -\chi_{61}$ (°)	77.5	75.9	74.7	76.8
$\chi_{31}, -\chi_{41}$ (°)	1.2	4.0	4.2	5.2

[a] Space group is $P1$ ($Z = 2$). Central torsion angle is $\phi_3 = 180°$ exactly, for symmetry reasons. The χ_{i1} angle is the torsion around the first C−C bond of the side chain connected to ring i. See also the caption to Table 1.

TABLE 7: Minimization Results for the Red Form of THT6[a]

	experiment	MM3-T-PDC	MM3-T-PDC-C6	MM3-T-DM
		Atoms Only		
Δ_{mol} (Å)		0.284	0.297	0.283
Δ_{cell} (Å)		0.539	0.312	0.535
F		0.044	0.048	0.034
ϕ_1, ϕ_5 (°)	178.2	156.7	155.4	157.3
ϕ_2, ϕ_4 (°)	178.2	160.0	155.0	156.0
ϕ_3 (°)	180.0	175.2	174.3	175.7
χ_{15}, χ_{65} (°)	67.8	71.5	70.7	71.6
χ_{35}, χ_{45} (°)	178.7	177.3	177.4	177.3
		Full Cell		
a (Å)	24.951	25.318	24.553	25.294
b (Å)	7.515	7.760	7.910	7.794
c (Å)	13.869	13.889	13.434	13.890
β (°)	117.244	116.400	115.65	116.55
ρ (g/cm^3)	1.192	1.127	1.171	1.125
Δ_{mol} (Å)		0.318	0.266	0.331
F		17.261	42.544	16.239
ϕ_1, ϕ_5 (°)	178.2	152.7	158.0	152.6
ϕ_2, ϕ_4 (°)	178.2	152.2	157.4	151.7
ϕ_3 (°)	180.0	174.9	175.8	175.3
χ_{15}, χ_{65} (°)	67.8	69.7	82.1	70.1
χ_{35}, χ_{45} (°)	178.7	178.2	178.4	178.2

[a] Space group adopted for the present minimizations is $C2$ (see the main text for a discussion). χ_{i5} angle is the torsion around the terminal C−C bond of the side chain connected to ring i. See also the caption to Table 1.

The red form of THT6 does not produce crystals suitable for single-crystal X-ray diffraction. Its unit cell was determined from powder diffraction spectra, supplementing the experimental data with ab initio periodic density functional theory (DFT) calculations.[25] The powder spectra could be equally well interpreted using either triclinic ($P1$) or monoclinic ($C2$ and $C2/m$) unit cells. DFT calculations were used to derive the atomic coordinates for the lower symmetry groups (at fixed lattice parameters) and predicted grater stability of the $C2$ unit cell (compared to $P1$). Eventually, the authors settled for a $C2/m$ cell with 50% occupancy of the lattice positions, due to room-temperature disorder of the terminal torsions of the alkyls. The ordered $C2$ group was adopted for our static energy minimizations.

Large displacements from the experimental positions are observed in the atoms-only minimizations on the red polymorph (see Δ_{cell} values in Table 7). However, this may be partly due to the fact that the atomic coordinates are actually the result of a theoretical calculation, having been obtained by DFT optimization. Hence, they do not necessarily or entirely reflect an inaccuary in the force field. Indeed, the lattice parameters from the full-cell minimizations are in excellent agreement with the experimental ones. The main-chain and side-chain torsion angles are also fairly close to experimental values. The performances of MM3-T-PDC and MM3-T-DM are very similar for this polymorph.

MD simulations of the yellow and red polymorphs of THT6 were also carried out with the MM3-T-PDC-C6 force field. The results in Table 3 were obtained with the previously derived optimal value for T4 ($C = 2.65$), without further adjustments. The average lattice parameters remain sufficiently close to experimental results. However, the densities are still too low. It seems that, despite the rescaling, we are still underestimating the van der Waals interactions for the present systems, at least in an average sense. In fact, we did not expect full transferability of our scaled C coefficients from T4 to other systems. Finally, visual inspection of the MD trajectories reveals dynamical disordering of the terminal methyls of the side chains, in qualitative agreement with the $C2/m$ cell model of red THT6.[25]

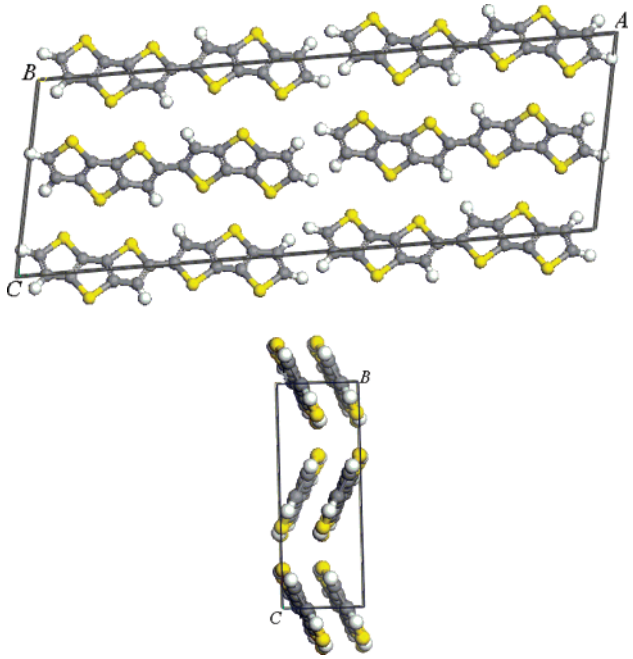

Figure 8. Two views of the unit cell of BDT (from MM3-T-PDC full-cell minimization).

Bis(dithienothiophene) (BDT). The packing of BDT is substantially different from that of the polymorphs of T4 or the other unsubstituted oligothiophenes.[22] There is no herringbone structure, but the molecules are arranged in layers of π-stacked molecules along the c axis (see Figure 8). Therefore, we considered this an interesting test for the point-charge versus distributed multipole models. Our results are collected in Table 8. We find that MM3-T-DM does better than MM3-T-PDC in the atoms-only minimizations but produced greater distortions of the lattice in the full-cell minimizations. Once more, note that the static energy minimizations with the standard MM3 van der Waals parameters predict densities that are too low, compared to the experimental room-temperature value.

TABLE 8: Minimization Results for BDT[a]

	experiment	MM3-T-PDC	MM3-T-DM
		Atoms Only	
Δ_{mol} (Å)		0.273	0.091
Δ_{cell} (Å)		0.114	0.101
F		3.841	2.523
		Full Cell	
a (Å)	33.689	34.043	33.365
b (Å)	3.883	4.125	3.855
c (Å)	11.106	11.621	12.262
β (°)	101.093	101.022	101.696
ρ (g/cm^3)	1.817	1.617	1.628
Δ_{mol} (Å)		0.165	0.238
F		71.255	119.990

[a] Space group is $C2/c$ ($Z = 2$). Central torsion angle is $\phi_1 = 180°$ exactly, for symmetry reasons. See also the caption to Table 1.

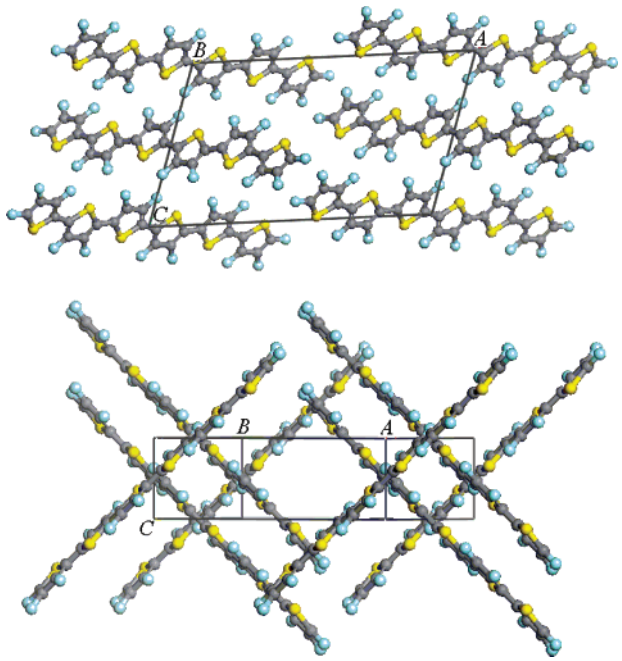

Figure 9. Two views of the unit cell of PFT6 (from MM3-T-DM full-cell minimization).

Perfluorosexithiophene (PFT6). The molecules of PFT6 are packed in a rather unusual fashion[23] (see Figure 9). Like BDT, they are arranged face-to-face in layers of π-stacked molecules. Adjacent molecules are shifted by one thiophene ring, so that two facing rings have opposite orientations, mutually canceling their dipole moments. However, the most interesting feature is that two successive layers are almost perpendicular to each other. Electrostatic interactions are largely responsible for this behavior. We were interested to see whether the point-charge model is sufficiently accurate to describe it, or a more sophisticated distributed multiple model is necessary in this case. Also, this represents a challenging test case, because intermolecular interactions involving fluorine are notoriously difficult to model accurately.

The results of our minimizations with MM3-T-PDC and MM3-T-DM are collected in Table 9. In both cases, we observe a ~10° distortion in the central torsions, in contrast to experimental results. This may be due to a slight incompatibility of the MM3 intramolecular equilibrium geometry with the experimental lattice. Atomic displacements in the atoms-only minimizations are comparable to those for the other molecules and, apparently, would seem to slightly favor the point-charge model. However, the distributed multipole model turns out to be clearly superior in the full-cell minimizations (compare the F values). This correlates nicely with the relatively poor fit of the molecular electrostatic potential, afforded by the point-change model (see the discussion at the end of the Force Fields section). The molecular packing and cell parameters remain rather close to the experimental ones. Also, the torsion angles become planar again, as they should be. There is no doubt that agreement with experimental values could be further improved by the ad hoc adjustment of a few bond distances and angles (using experimental or ab initio values, instead of those provided by MM3) and some rescaling/modification of the van der Waals parameters. However, we were satisfied with the qualitative result, and did not try to pursue this approach further.

TABLE 9: Minimization Results for PFT6[a]

	experiment	MM3-T-PDC	MM3-T-DM
		Atoms Only	
Δ_{mol} (Å)		0.142	0.176
Δ_{cell} (Å)		0.188	0.200
F		0.245	0.480
ϕ_1, ϕ_5 (°)	178.3	179.4	179.8
ϕ_2, ϕ_4 (°)	178.4	171.9	168.7
		Full Cell	
a (Å)	18.549	21.427	20.448
b (Å)	5.323	4.502	5.107
c (Å)	13.214	13.169	12.269
β (°)	108.631	101.302	107.547
ρ (g/cm^3)	2.004	1.988	2.028
Δ_{mol} (Å)		0.108	0.097
F		561.816	212.703
ϕ_1, ϕ_5 (°)	178.3	178.9	177.1
ϕ_2, ϕ_4 (°)	178.4	178.5	179.5

[a] Space group is $P2_1/c$ ($Z = 2$). Central torsion angle is $\phi_3 = 180°$ exactly, for symmetry reasons. See also the caption to Table 1.

Conclusions

Apart from an early attempt by Ferro et al.,[32] which employed an MM2-type force field with relatively crude electrostatics (dipoles on C−S bonds only) and yielded only partially satisfactory results, this is the first systematic molecular modeling study of the crystal structures of oligothiophenes. We have considered several systems and polymorphs, spanning a whole range of molecular packing modes.[7,13,19−25] We have also investigated different electrostatic models, including potential-derived charges (PDC)[33] or atom-centered charges, dipoles, and quadrupoles.[35−37] Although limited to one specific set of compounds, our study is similar to that of Leusen et al.,[48] who recently considered different electrostatic models and their ability to reproduce the crystal structures of a number of pharmaceutical compounds. They observed that distributed multipoles performed better than point charges for rigid molecules, but the latter were superior for flexible molecules. One of our main conclusions is that, at least in most of the present cases, the distributed multipole model does not present a clear advantage over the simpler point-charge model: It may be slightly worse or slightly better, but in any case, the additional computational cost does not appear to be justified. There is one notable exception, however. Perfluorinated tetrathiophene has a rather unusual crystal structure, which is modeled correctly only by using the atom-based distributed multipoles. This agrees with the poor fit of the gas-phase molecular electrostatic potential afforded by the point-charge model (33% relative error, in this particular case).

In addition to the lattice energy minimizations, we also performed some room-temperature molecular dynamics simula-

tions of the crystals with the point-charge force field. This is more rigorously correct than using minimized structures when comparing to X-ray structures obtained at room temperature. We found that the standard MM3 exp-6 parameters for H, C, and S lead to crystal densities that are too low (typically by ~10%), after inclusion of the thermal motion. This forced us to modify the van der Waals parameters. After some trial and error, all C_6 dispersion coefficients were homogeneously increased by a factor of 1.151, leading to the correct room-temperature densities (but also to slightly overestimated heats of sublimation for T4 and T6). Naturally, ours was only one among many possible options. Fine-tuning of specific nonbonded parameters could have led to results that were equally good or better. Nonetheless, we may certainly conclude that, while the MM3 nonbonded parameters appear to be adequate for the static simulations of organic crystals (they were designed for this purpose, like the subsequent MM4 force field[49]), some modifications/rescaling are necessary for MD simulations.

The atomic charges or multipoles were always calculated in the trans planar conformations (i.e., identical or very close to the ones observed in the crystals). In principle, the molecular charge distribution can depend on the conformational state. This may be accounted for either in a purely empirical way by an explicit dependence of the charges or multipoles on the torsion angles[50] or at a more fundamental level by the inclusion in the force field of intra- and intermolecular polarization effects.[28] Here, we avoided the introduction of this additional complication, also, because comparison with the crystal structures is not expected to provide a critical test of the goodness of the model adopted for the conformation dependence of the charge distribution. Nonetheless, this question and the associated one of the inclusion of polarization effects in an approximate force field for conjugated systems is an interesting one, and we plan to return to it in the future by a combination of ab initio and force field calculations.

Finally, we believe that the present MM3-T-PDC-C6 force field for unsubstituted and alkyl-substituted oligothiophenes provides a reasonably good balance between accuracy and simplicity of the description. We plan to apply it to a number of interesting problems, including the structure and molecular motions in odd oligothiophenes (T5 and T7), the structure of poly(alkylthiophenes), and the structure, energetics, and growth of the T4 crystal surfaces.

Acknowledgment. We thank several people in the Milan area for discussions and encouragement: G. Allegra, P. Arosio, D. Ferro, A. Gavezzotti, S. V. Meille, M. Moret, and W. Porzio. Correspondence with N. L. Allinger is also gratefully acknowledged. This work was financially supported by the PRIN03 program by MIUR.

Supporting Information Available: One PDF file containing: (a) graphical comparison of common van der Waals potentials (Buckingham or Lennard-Jones) for C···C, C···S, and S···S interactions; (b) the optimized atomic coordinates (B3LYP/6-31G**) and distributed multipoles of T4, BDT, and PFT4, in the global molecular reference frame (*GAMESS-USA* output) and in the atom-based local reference frame (*TINKER* input). Four text-only files containg Tinker-style parameter definitions for T4, BDT, PFT4, and THT6, for the MM3-T-PDC and MM3-T-DM force fields.

References and Notes

(1) Garnier, F. *Acc. Chem. Res.* **1999**, *32*, 209.
(2) Cornil, J.; Beljonne, D.; Calbert, J.-P.; Brédas, J.-L. *Adv. Mater.* **2001**, *13*, 1053.
(3) Katz, H. E.; Bao, Z. *J. Phys. Chem. B* **2000**, *104*, 671.
(4) Dimitrakopoulos, C. D.; Malefant, P. R. L. *Adv. Mater.* **2002**, *14*, 99.
(5) Köhler, A.; Wilson, J. S.; Friend, R. H. *Adv. Mater.* **2002**, *14*, 701.
(6) *Handbook of Oligo- and Polythiophenes*; Fichou, D., Ed.; Wiley-VCH: Weinheim, Germany, 1999.
(7) Fichou, D. *J. Mater. Chem.* **2000**, *10*, 571.
(8) Mena-Osteritz, E. *Adv. Mater.* **2002**, *14*, 609.
(9) Torsi, L.; Tanese, M. C.; Cioffi, N.; Gallazzi, M. C.; Sabbatini, L.; Raos, G.; Meille, S. V.; Giangregorio, M. M. *J. Phys. Chem. B* **2003**, *107*, 7589.
(10) Mikkelsen, K.; Ratner, M. A. *Chem. Rev.* **1987**, *87*, 113. Bromley, S. T.; Mas-Torrent, M.; Hadley, P.; Rovida, C. *J. Am. Chem. Soc.* **2004**, *126*, 6544.
(11) Desiraju, G. R. *Angew. Chem., Int. Ed. Engl.* **1995**, *34*, 2311.
(12) Gavezzotti, A. *Modell. Simul. Mater. Sci. Eng.* **2002**, *10*, R1.
(13) Curtis, M. D.; Cao, J.; Kampf, J. W. *J. Am. Chem. Soc.* **2004**, *126*, 4318.
(14) Brédas, J.-L.; Cornil, J.; Beljonne, D.; Dos Santos, D. A.; Shuai, Z. *Acc. Chem. Res.* **1999**, *32*, 267.
(15) Salzner, U.; Kızıltepe, T. *J. Org. Chem.* **1999**, *64*, 764.
(16) Raos, G.; Famulari, A.; Meille, S. V.; Gallazzi, M. C.; Allegra, G. *J. Phys. Chem. A* **2004**, *108*, 691.
(17) Mattheus, C. C.; de Wijs, G. A.; de Groot, R. A.; Palstra, T. T. M. *J. Am. Chem. Soc.* **2003**, *125*, 6323.
(18) Day, G. M.; Price, S. L. *J. Am. Chem. Soc.* **2003**, *125*, 16434.
(19) Porzio, W.; Destri, S.; Mascherpa, M.; Brückner, S. *Acta Polym.* **1993**, *44*, 266.
(20) Siegrist, T.; Kloc, C.; Laudise, R. A.; Katz, H. E.; Haddon, R. C. *Adv. Mater.* **1998**, *10*, 379. Antolini, L.; Horowitz, G.; Kuoki, F.; Garnier, F. *Adv. Mater.* **1998**, *10*, 382.
(21) Horowitz, G.; Bachet, B.; Yassar, A.; Lang, P.; Demanze, F.; Fave, J. L.; Garnier, F. *Chem. Mater.* **1995**, *7*, 1337. Siegrist, T.; Fleming, R. M.; Haddon, R. C.; Laudise, R. A.; Lovinger, A. J.; Katz, H. E.; Bridenbaugh, P.; Davis, D. *J. Mater. Res.* **1995**, *10*, 2170.
(22) Li, X.-C.; Sirringhaus, H.; Garnier, F.; Holmes, A. B.; Moratti, S. C.; Feeder, N.; Clegg, W.; Teat, S. J.; Friend, R. H. *J. Am. Chem. Soc.* **1998**, *120*, 2206.
(23) Sakamoto, Y.; Komatsu, S.; Suzuki, T. *J. Am. Chem. Soc.* **2001,** *123*, 4643.
(24) Destri, S.; Ferro, D. R.; Khotina, I. A.; Porzio, W.; Farina, A. *Macromol. Chem. Phys.* **1998**, *199*, 1973.
(25) Neumann, M. A.; Tedesco, C.; Destri, S.; Ferro, D. R.; Porzio, W. *J. Appl. Crystallogr.* **2002**, *35*, 296.
(26) Meille, S. V.; Romita, V.; Caronna, T.; Lovinger, A. J.; Catellani, M.; Belobrzeckaja, L. *Macromolecules* **1997**, *30*, 7898.
(27) Allinger, N. L.; Yuh, Y. H.; Li, J.-H. *J. Am. Chem. Soc.* **1989**, *111*, 8551. Li, J.-H.; Allinger, N. L. *J. Am. Chem. Soc.* **1989**, *111*, 8566 and 8576.
(28) Ponder, J. W. *TINKER: Software Tools for Molecular Design*, 4.1 ed.; Washington University School of Medicine: Saint Louis, MO, 2003.
(29) Ren, P.; Ponder, J. W. *J. Comput. Chem.* **2002**, *23*, 1497; *J. Phys. Chem. B* **2003**, *107*, 5933. Pappu, R. V.; Hart, R. K.; Ponder, J. W. *J. Phys. Chem. B* **1998**, *102*, 9725. Hodsdon, M. E.; Ponder, J. W.; Cistola, D. P. *J. Mol. Biol.* **1996**, *264*, 585. Kundrot, C. E.; Ponder, J. W.; Richards, F. M. *J. Comput. Chem.* **1991**, *12*, 402. Ponder, J. W.; Richards, F. M. *J. Comput. Chem.* **1987**, *8*, 1016.
(30) Yang, L.; Allinger, N. L. *THEOCHEM* **1996**, *370*, 71.
(31) Raos, G.; Famulari, A.; Marcon, V. *Chem. Phys. Lett.* **2003**, *379*, 364.
(32) Ferro, D. R.; Porzio, W.; Destri, S.; Ragazzi, M.; Brückner, S. *Macromol. Theory Simul.* **1997**, *6*, 713.
(33) Spackman, M. A. *J. Comput. Chem.* **1996**, *17*, 1.
(34) Schmidt, M. W.; Baldridge, K. K.; Boatz, J. A.; Elbert, S. T.; Gordon, M. S.; Jensen, J. H.; Koseki, S.; Matsunaga, N.; Nguyen, K. A.; Su, S. J.; Windus, T. L.; Dupuis, M.; Montgomery, J. A. *J. Comput. Chem.* **1993**, *14*, 1347.
(35) Stone, A. J. *The Theory of Intermolecular Forces*; Clarendon Press: Oxford, 1996.
(36) Price, S. L. *J. Chem. Soc., Faraday Trans.* **1996**, *92*, 2997.
(37) Williams, D. E. *J. Comput. Chem.* **1988**, *9*, 745.
(38) Marcon, V.; Raos, G.; Allegra, G. *Macromol. Theory Simul.* **2004**, *13*, 497.
(39) Materials Studio and Discover are products of Accelrys Inc. (http://www.accelrys.com).
(40) Leach, A. R. *Molecular Modelling: Principles and Application*, 2nd ed.; Prentice Hall, London, 2001.
(41) Field, M. J. *A Practical Introduction to the Simulations of Molecular Systems*; Cambridge University Press: Cambridge, U.K., 1999.
(42) Williams, D. E. *PCK83*. Quantum Chemistry Program Exchange, program no. 548.

(43) The rotation angle $\Delta\phi$ is defined as follows. Let $\mathbf{A} = [a_{ij}]$ be the rotation matrix bringing the old axes into the new axes of inertia. Then, $\Delta\phi = \arccos[1/2(\sum a_{ij} - 1)]$.

(44) Filippini, G.; Gavezzotti, A. *Acta Cryst.* **1993**, *B49*, 868.

(45) Berendsen, H. J. C.; Postma, J. P. M.; van Gunsteren, W. F.; Di Nola, A.; Haak, J. R. *J. Chem. Phys.* **1984**, *81*, 3684.

(46) Kloc, Ch; Laudise, R. A. *J. Cryst. Growth* **1998**, *193*, 563.

(47) Jorgensen, W. L.; Maxwell, D. S.; Tirado-Rives, J. *J. Am. Chem. Soc.* **1996**, *118*, 11225.

(48) Brodersen, S.; Wilke, S.; Leusen, F. J. J.; Engel. G. *Phys. Chem. Chem. Phys.* **2003**, *5*, 4923.

(49) Allinger, N. L.; Chen, K.; Lii, J. H. *J. Comput. Chem.* **1996**, *17*, 642.

(50) Koch, U.; Stone, A. J. *J. Chem. Soc., Faraday Trans.* **1996**, *92*, 1701.